Table III. Methanolysis Products in 50% Aqueous Methanol in the Presence of 2,6-Lutidine (55 °C)

substrate	methyl arylphosphonate (product) $\delta(CH_3)^a$	$\delta(CH_2)^a$	R_f^b	yield,[c] %
1	3.55 (d, 3 H)		0.62	49
2	3.35 (d, 3 H)	3.52 (d, 2 H)	0.64	50
3	3.10 (d, 3 H)	3.60 (d, 2 H)	0.67	39
4	3.53 (d, 3 H)		0.72	42

[a] ^1H NMR signal in D_2O; from sodium 2,2-dimethyl-2-silapentane-5-sulfonate. [b] Toyo Filter Paper No. 50; *n*-PrOH–NH_3 (28%)–H_2O (6:3:1). [c] Based on NMR analysis.

Kinetic Measurements. All of the rates were determined under pseudo-first-order conditions.

(a) In the Absence of Metal Ion. The reaction mixture (substrate = 0.01 M, and μ = 1.0 (KCl)) was transferred into ampules and kept in a constant temperature bath. The hydrolysis rate was then determined by monitoring the amounts of inorganic sulfate released at appropriate time intervals according to the barium chloranilate method previously reported.[7-9]

(b) In the Presence of Metal Ion. 2-(*N*-Morpholine)ethanesulfonic acid–NaOH (0.1 M) was used as the buffer. In the presence of $Mg(NO_3)_2$, the kinetic method was exactly the same as described above. In the presence of $Zn(NO_3)_2$, two methods were employed. (1) The barium chloranilate method was applied to the cases of phenyl- (**3**) and benzylphosphonosulfate (**4**), for which a sample solution (5 mL) for analysis was composed of the reaction mixture (0.5 mL), acetate buffer (1 mL, 2.5 M, pH 4), an ethanol solution of 8-hydroxyquinoline (2.5 mL, 6×10^{-3} M), and water. This composition is the same as that employed for usual analysis except for the presence of 8-hydroxyquinoline. (2) In the cases of 2-pyridyl- (**1**) and 2-pyridylmethylphosphonosulfate (**2**), the rates were followed by means of high-pressure liquid chromatography [HPLC Yanako L-2000; column, Yanako PEL-AX (o.d. 2 mm × 500 mm); eluant, 5×10^{-2} M KH_2PO_4; sample size, 4 μL]; a phosphonate produced during the reaction was well separated from the corresponding phosphonosulfate. Method 1 was also applied to the latter cases.

Product Analysis. (a) Hydrolysis. Amounts of the liberated inorganic sulfate were determined colorimetrically by using barium chloranilate as mentioned above. Phosphonates were identified by paper chromatography and their yields were evaluated on the basis of UV absorption intensity (Table I). In the cases of **1** and **2** the phosphonates could be accurately determined by high-pressure liquid chromatography as mentioned above.

(b) Methanolysis in the Absence of Metal Ion. (1) Under Acidic Conditions in 50% Aqueous Methanol (55 °C). The reaction mixtures were neutralized to pH 7 and concentrated to dryness. Dried solid residues were analyzed by NMR in D_2O for methyl sulfate: $\delta(CH_3)$ (D_2O) 3.73 (3 H, singlet).

(2) Under Neutral pH Conditions in 50% Aqueous Methanol (55 °C). 2-Pyridylmethylphosphonosulfate (**2**) (150 mg) was dissolved in 50% aqueous methanol containing 2,6-lutidine (1 M) to prepare its 0.1 M solution. The reaction mixture was kept for 24 h at 55 °C and concentrated to dryness. The solid residue was dissolved in 5 mL of water, to which was added a few drops of aqueous ammonia (28%). This aqueous solution was again evaporated to dryness, and the residue was dried on P_2O_5 and analyzed by NMR in D_2O for methyl 2-pyridylmethylphosphonate. This ester was also analyzed by paper and high-pressure liquid chromatography. The results including those for other substrates are shown in Table III.

(c) Methanolysis in the Presence of $Zn(NO_3)_2$ in 50% Aqueous Methanol (55 °C). The reaction gave essentially the same results as described above for the case without metal ion as regards product distribution. In all the cases including that of Cu^{2+} ion, the formation of methyl sulfate was not detected.

Acknowledgment. We are grateful to Professor Y. Murakami of Kyushu University, Japan, for his helpful discussions and comments. This research was supported in part by a Grant-in-Aid for Environmental Science from the Ministry of Education, Science, and Culture, Japan.

Registry No. 1, 80642-94-0; **2**, 80642-95-1; **3**, 80642-96-2; **4**, 80642-97-3; **5**, 32599-82-9; 2-pyridylphosphonate diammonium salt, 80642-98-4; 2-pyridylmethylphosphonate diammonium salt, 80642-99-5; phenylphosphonate diammonium salt, 63119-09-5; benzylphosphonate diammonium salt, 80643-00-1; methyl 2-pyridylphosphonate, 80643-01-2; methyl 2-pyridylmethylphosphonate, 80643-02-3; methyl phenylphosphonate, 10088-45-6; methyl benzylphosphonate, 63581-66-8; Zn, 7440-66-6; Mg, 7439-95-4.

Studies of Hydrogen-Bonded 5′-Guanosine Monophosphate Self-Associates Using Low-Frequency Raman Scattering

O. Faurskov Nielsen,* P.-A. Lund, and Steffen B. Petersen

Contribution from the Chemical Laboratory V, H. C. Ørsted Institute, University of Copenhagen, 5 Universitetsparken, DK-2100 Copenhagen, Denmark. *Received September 8, 1981*

Abstract: The temperature and concentration dependence of the low-frequency (20–400 cm^{-1}) Raman spectra of the disodium and dipotassium salt in the gel state have been studied by calculation of $R(\bar{\nu})$. The spectra showed two bands below 150 cm^{-1} with maxima at ca. 115 and ca. 80 cm^{-1}, respectively. The former is assigned to hydrogen-bonded self-associates of 5′-GMP, whereas the latter is ascribed to non-hydrogen-bonded self-associates or monomers of 5′-GMP. The gel state spectra did only differ from the solution spectra by a drastically increased intensity of the band at ca. 115 cm^{-1}, indicating that hydrogen-bonded self-associates are the dominant species in the gel state. The effect of deuterium substitution (N–D and O–D) upon the spectra was insignificant.

We compared[1,2] low-frequency Raman scattering (Rayleigh-wing scattering) to far-infrared absorption for a number of molecular liquids by calculation of $R(\bar{\nu})$ from the scattered intensity in Stoke's side. The absorption coefficient for water is very high in the far-IR region, and absorption spectra of water and aqueous solutions are thus difficult to obtain. The high intensity of the central (exciting) line makes it in practice nearly impossible to investigate Raman spectra of aqueous solutions below 200 cm^{-1}. The main advantage of the $R(\bar{\nu})$ technique is that the central line in a Raman spectrum is suppressed and the low-frequency vibrations thus much easier observed. This fact was demonstrated in our low-frequency studies of water[3] and of aqueous solutions

(1) Lund, P. A.; Nielsen, O. F.; Praestgaard, E. *Chem. Phys.* **1978**, *28*, 167–173.

(2) Nielsen, O. F.; Christensen, D. H.; Lund, P.-A.; Praestgaard, E. Proceedings of the 6th International Conference on Raman Spectroscopy, Bangalore, India, 1978; Heyden and Son: London, Philadelphia, Rheine, 1978; Vol. 2, pp 208–209.

(3) Nielsen, O. F. *Chem. Phys. Lett.* **1979**, *60*, 515–517.

0002-7863/82/1504-1991$01.25/0

of γ-aminobutyric acid,[4] of mononucleosides[5,6] and mononucleotides[7] and of amides.[8] Even low-frequency spectra of aqueous gels were obtained by this technique.[6,9]

Aqueous solutions of mononucleosides[5,6] and mononucleotides[7] both give rise to a band between 50 and 100 cm^{-1} in the $R(\bar{\nu})$ curves. This band is sensitive to protonization of the base moiety, and since neither pure water[3] nor aqueous salt solutions[10] show this band, it was suggested that the vibrational mode responsible for this band involved a hydrogen bond between the base and the solvent. A preliminary study[10] of the cation dependence of the low-frequency bands of 5′-guanosine monophosphate (5′-GMP) supported this interpretation.

It is well-known, mainly from NMR studies, that 5′-GMP forms highly ordered self-associates when dissolved in water.[11-15] Both hydrogen bonding and stacking between different units of 5′-GMP are stabilizing the structures in solution at pH ca. 8. The exchange rates in this system[11] are sufficiently low to permit a direct comparison of Raman and NMR studies, and thus this system is particular well suited for testing if hydrogen bonds are the cause of the observed low-frequency bands.

Brooker, Perrot, and Lascombe[16-19] used the high-frequency or low-temperature approximation for $R(\bar{\nu})$ in studies of molecular liquids, water, and aqueous solutions of inorganic salts. In our investigations of aqueous solutions of biological molecules, we found it necessary to perform a background correction.[3-10,20] In this paper the importance of this correction for the $R(\bar{\nu})$ representation will be discussed.

Experimental Section

Chemicals and Sample Preparation. The sodium salt of 5′-GMP·4.5H_2O was obtained from SIGMA. The potassium salt was prepared and dried as previously described.[10] Five different concentrations of the sodium salt were prepared by dissolving 194, 155, 117, 78, and 39 mg of Na_2-5′-GMP·4.5H_2O in 700 μL of redistilled water each, and five different concentrations of K_2-5′-GMP were obtained by dissolving 175, 140, 105, 70, and 35 mg of K_2-5′-GMP in 700 μL of redistilled water each. The approximative molarities of 5′-GMP in corresponding solutions of the sodium and potassium salts are as follows: 0.57, 0.45, 0.34, 0.23, and 0.11 M. The pHs in these solutions ranged from 8.4 (high concentration) to 7.8 (low concentration). In the 0.11 M solution of K_2-5′-GMP some precipitation was observed. All solutions were cleaned for dust and other particles by ultracentrifugation at 65.000–100.000 rpm using a Beckman Airfuge ultracentrifuge. Particles were effectively removed from the solutions, and samples well suited for light scattering were obtained. Approximately 350 μL of each solution was transferred to a 10-mm (o.d.) NMR tube which was used as a cell.

The gelified Na_2-5′-GMP samples were prepared by adding 4 M HCl dropwise to the 0.11, 0.23, and 0.34 M solutions. These gels were then melted by heating on a water bath, and upon being cooled rather transparent gels formed. Gels of the more concentrated solutions were not investigated because the tranparencies were too low. Gels of the potassium salt could not be prepared because precipitation transparencies at temperatures above ca. 50 °C.

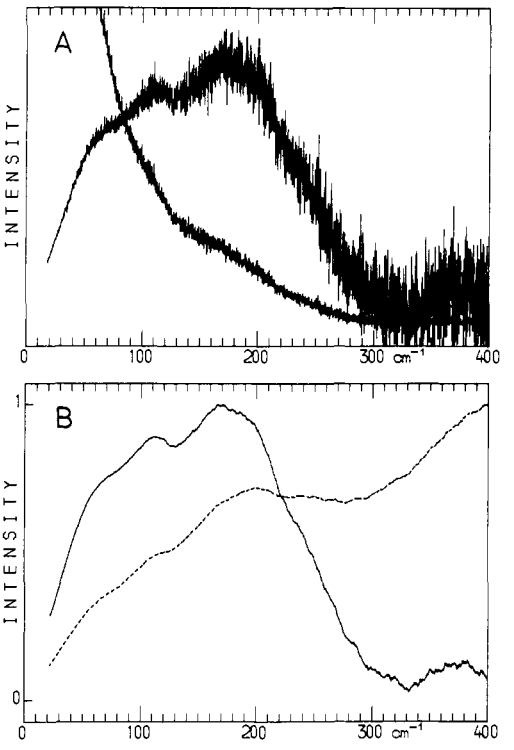

Figure 1. A shows the low-frequency Raman spectrum, $I(\bar{\nu})$, of a 0.23 M aqueous solution of K_2-5′-GMP. The $R(\bar{\nu})$ curve is constructed directly from these data by using background correction; see text. B shows the smoothed version of the $R(\bar{\nu})$ curve in A (full line). B also shows another $R(\bar{\nu})$ curve (dotted line) constructed as above but without background correction. The highest intensity in a given $R(\bar{\nu})$ curve in B was normalized to 1.

Deuterated samples were prepared by exchange with D_2O (Norsk Hydro, 99.8 atom % D). Either 0.5 g of K_2-5′-GMP or Na_2-5′-GMP were treated at room temperature with 5 mL of D_2O, and D_2O was then evaporated in vacuo. This treatment was repeated four times for each sample. The samples were dried in vacuo. More than 95% of the exchangeable hydrogen atoms were substituted by deuterium according to the ^1H NMR spectra. A 175-mg sample of the deuterated potassium salt and 194 mg of the deuterated sodium salt were each dissolved in 700 μL of D_2O. The molarities of the samples are 0.5–0.6. Both samples were ultracentrifuged prior to use.

Instrumental. Raman spectra from 20 to 400 cm^{-1} were recorded on a Coderg PH1 spectrometer using 90° scattering. The detector was a cooled PM tube (EMI 9558), equipped with a Coderg CPH 100 photon counting system. The scattering plane was horizontal and the 514.5-nm line, vertically polarized, of a Spectra-Physics 165 Ar^+ laser was used as exciting source. The laser power was 400 mW, and the registration speed was 10 cm^{-1}/min. Scattering in I_{VH} configuration was measured by means of a polaroid sheet followed by a quarter wave plate in the scattered beam. The reason for this choice of configuration is the minor intensity of the exciting line in comparison to the I_{VV} configuration. Although exact depolarization ratios were difficult to obtain, measurements on a few selected samples showed that all the bands observed seemed to be depolarized and thus no information was lost in the I_{VH} configuration. The number of counts per step in frequency (8.4 step/cm^{-1}) was sampled by a microprocessor unit and fed to an RC 4000 computer. The dynamical range was 24 bits.

The samples were heated and cooled by means of thermostated water or alcohol baths circulated through copper tubings around the cells. The temperature accuracy at the sample was estimated to ±1 °C.

Results and Discussion

Construction of $R(\bar{\nu})$ Curves. The $R(\bar{\nu})$ curves were calculated from the intensity in Stoke's side of the Raman spectrum, $I(\bar{\nu})$.

$$R(\bar{\nu}) \propto \bar{\nu}[1 - \exp(-h\bar{\nu}c/kT)]I(\bar{\nu})$$

(4) Nielsen, O. F. *Chem. Phys. Lett.* **1979**, *66*, 350–352.
(5) Nielsen, O. F.; Lund, P.-A.; Praestgaard, E. *J. Raman Spectrosc.* **1980**, *9*, 286–290.
(6) Nielsen, O. F.; Lund, P.-A.; Nicolaisen, F. M. and Praestgaard, E. Proceedings of the 7th International Conference on Raman Spectroscopy, Ottawa, Canada, 1980, North-Holland Publishing Co.: Amsterdam, 1980; pp 480–481.
(7) Nielsen, O. F.; Lund, P.-A.; Praestgaard, E. *J. Raman Spectrosc.* **1981**, *11*, 92–95.
(8) Nielsen, O. F.; Lund, P.-A. *Chem. Phys. Lett.* **1981**, *78*, 626–628.
(9) Nielsen, O. F.; Lund, P.-A.; Nicolaisen, F. M. *Acta Chem. Scand., Ser. A* **1980**, *A34*, 749–754.
(10) Nielsen, O. F.; Lund, P.-A.; Petersen, S. B. *J. Raman Spectrosc.* **1981**, *11*, 493–495.
(11) Detellier, C.; Laszlo, P. *Helv. Chim. Acta* **1979**, *62*, 1559–1565 and references cited therein.
(12) Pinnavaia, T. J.; Marshall, C. L.; Mettler, C. M.; Fisk, C. L.; Miles, H. T.; Becker, E. D. *J. Am. Chem. Soc.* **1978**, *100*, 3625–3627.
(13) Borzo, M.; Detellier, C.; Laszlo, P.; Paris, A.; *J. Am. Chem. Soc.* **1980**, *102*, 1124–1134 and references cited therein.
(14) Detellier, C.; Laszlo, P. *J. Am. Chem. Soc.* **1980**, *102*, 1135–1141 and references cited therein.
(15) Petersen, S. B.; Led, J. J.; Grant, D. M., submitted for publication in *J. Am. Chem. Soc.*
(16) Brooker, M. H.; Perrot, M. *J. Mol. Struct.* **1980**, *60*, 317–320.
(17) Perrot, M.; Brooker, M. H.; Lascombe, J. *J. Chem. Phys.* **1981**, *74*, 2787–2794.
(18) Brooker, M. H.; Perrot, M. *J. Chem. Phys.* **1981**, *74*, 2795–2799.
(19) Perrot, M.; Bouachir, M.; Lascombe, J. *Mol. Phys.* **1981**, *42*, 551–564.
(20) Nielsen, O. F.; Lund, P.-A.; Praestgaard, E. *J. Chem. Phys.* **1981**, *75*, 1586–1587.

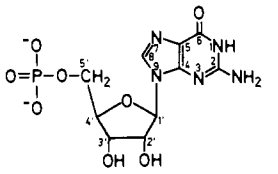

Figure 2. The dominant molecular species of 5'-GMP at pH ca. 8.

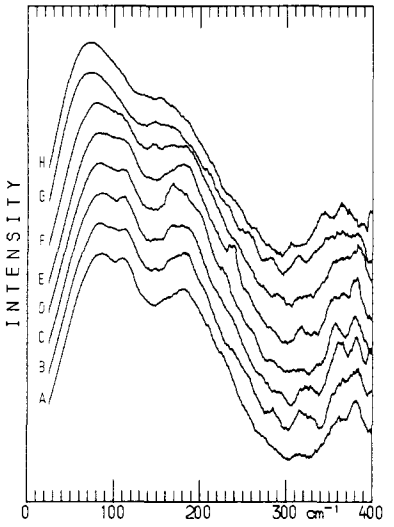

Figure 3. $R(\bar{\nu})$ curves for 0.57 M aqueous solutions of Na_2-5'-GMP at different temperatures. At room temperature the pH was measured to 8.3: A, −2 °C, B, 1 °C, C, 6 °C, D, 11 °C, E, 16 °C, F, 25 °C, G, 40 °C, H, 51 °C. The highest intensity in a given $R(\bar{\nu})$ curve was normalized to 1.

$\bar{\nu}$ is the Raman shift in cm^{-1}, h is Planck's and k is Boltzmann's constant, T is the absolute temperature, and c is the velocity of light. The influence of differences in monochromator response and the ν^4 dependence is neglected because the influence of these factors is very small in this limited frequency region. The background corrections in which we subtract a mean intensity value found in a 10-cm^{-1} interval around the lowest intensity values prior to calculation of $R(\bar{\nu})$ have proven very useful in earlier studies of biological molecules as well as in the present study. However, the background correction has given rise to some discussions[18,20] therefore, we shall illustrate the effect of the correction in one of the $R(\bar{\nu})$ curves.

In Figure 1A is shown the low-frequency Raman spectrum ($I(\bar{\nu})$) of a 0.23 M aqueous solution of K_2-5'-GMP together with the $R(\bar{\nu})$ curve constructed after the background correction has been performed. The smoothed $R(\bar{\nu})$ curve corresponding to the curve in Figure 1A are given in Figure 1B as well as a smoothed $R(\bar{\nu})$ curve calculated from the $I(\bar{\nu})$ curve in Figure 1A but without any background correction. As seen from Figure 1B the low-frequency features below ca. 150 cm^{-1} are much easier observed in the $R(\bar{\nu})$ curve with background correction than in the curve without. However, a disadvantage is that the relative intensities in the $R(\bar{\nu})$ curves may be influenced by this correction, especially at frequencies higher than ca. 150 cm^{-1}. Background corrections in the way outlined above are performed for the $R(\bar{\nu})$ curves given in the rest of this paper. The highest intensity in a given $R(\bar{\nu})$ curve is normalized to 1, and thus only relative intensities between bands in the $R(\bar{\nu})$ curves should be compared.

Aqueous Solutions at pH ca. 8. The dominant molecular species of 5'-GMP in aqueous solutions at pH ca. 8 is given in Figure 2. The dependence upon temperature of the $R(\bar{\nu})$ curves for the 0.57 M 5'-GMP solutions (ca. 0–50 °C) is shown in Figure 3 for the sodium salt and in Figure 4 for the potassium salt. In all solutions a band around 180 cm^{-1} is observed. As seen from Figures 3 and 4 the shape and the frequency maximum for this band shift only a little from one temperature to another. This band arises from external water modes as previously described.[3] Brooker et al. reported[16,18] that the $R(\bar{\nu})$ curve for water changed

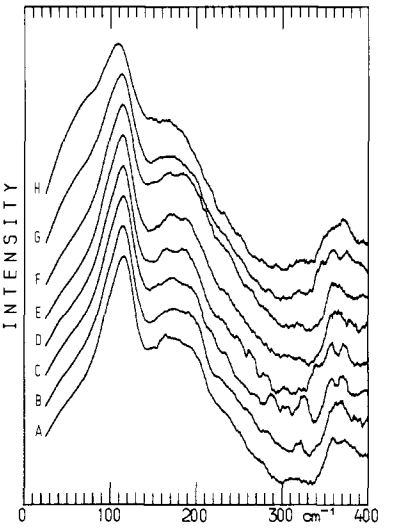

Figure 4. $R(\bar{\nu})$ curves for 0.57 M aqueous solutions of K_2-5'-GMP at different temperatures. At room temperature the pH was measured to 8.2: A, −3 °C, B, 1 °C, C, 6 °C, D, 11 °C, E, 16 °C, F, 24 °C, G, 40 °C, **H**, 50 °C. The highest intensity in a given $R(\bar{\nu})$ curve was normalized to one.

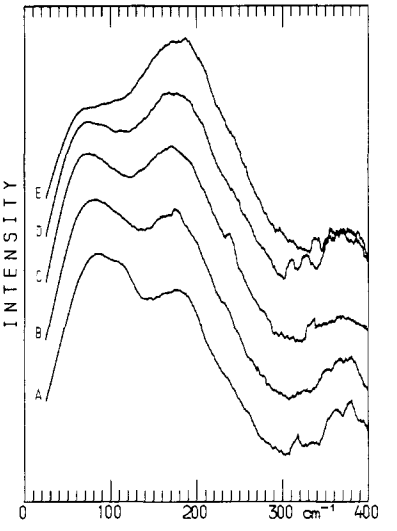

Figure 5. $R(\bar{\nu})$ curves of Na_2-5'-GMP at different concentrations in aqueous solutions at 22 °C and pH 7.8–8.4: A, 0.57 M, B, 0.45 M, C, 0.34 M, D, 0.23 M, E, 0.11 M. The highest intensity in a given $R(\bar{\nu})$ curve was normalized to 1.

only slowly with temperature. Temperature experiments in our laboratory confirm this slow temperature dependence.

The most intense band observed in solutions of Na_2-5'-GMP (Figure 3) is found at 87 cm^{-1} at −2 °C, and at 51 °C this band is shifted to 70 cm^{-1}. With gradually increasing temperature the band shifts continuously from the higher to the lower limit of this frequency interval. Another very weak band with a maximum between 110 and 120 cm^{-1} is observed in the $R(\bar{\nu})$ curve at 25 °C in Figure 3. This band disappears at temperatures above 25 °C, but it gains intensity relative to the more intense band at 70–87 cm^{-1} as the temperature is lowered.

The band of highest intensity in the solution of K_2-5'-GMP in Figure 4 is found at 118 cm^{-1} at −3 °C and at 110 cm^{-1} at 50 °C. As the temperature increases from −3 to 50 °C, the maximum for this band is gradually shifted from 118 to 110 cm^{-1}. The band is asymmetric and possibly shows a shoulder at ca. 100 cm^{-1} in the $R(\bar{\nu})$ curves obtained at the lowest temperatures. At 50, 40, and 24 °C an additional broad, weak band is observed as a shoulder at ca. 70 cm^{-1}.

Figure 5 shows the dependence upon concentration of Na_2-5'-GMP in aqueous solutions. All spectra were obtained at temperatures between 21 and 22 °C. The most concentrated solution

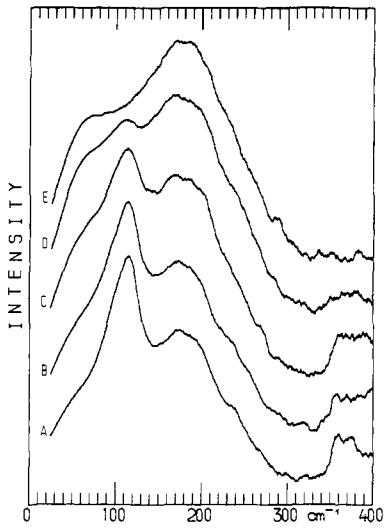

Figure 6. $R(\bar{\nu})$ curves of K_2-5′-GMP at different concentrations in aqueous solutions at 22 °C and pH 7.8–8.4; A, 0.57 M, B, 0.45 M, C, 0.34 M, D, 0.23 M, E 0.11 M. The highest intensity in a given $R(\bar{\nu})$ curve was normalized to 1.

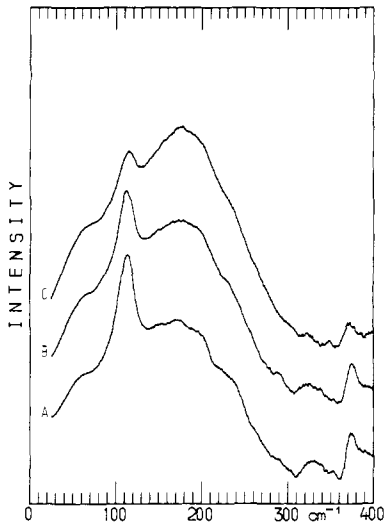

Figure 7. $R(\bar{\nu})$ curves of Na_2-5′-GMP at different concentrations at pH 4–5 and 22 °C: A, 0.34 M, B, 0.23 M, C, 0.11 M.

(0.57 M) shows a weak band with maximum at ca. 112 cm^{-1}. This band may possibly remain in the 0.45 M solution but has completely disappeared in the 0.34, 0.23, and 0.11 M solutions. All solutions exhibit a broad band with a maximum between ca. 70 and 85 cm^{-1}.

$R(\bar{\nu})$ curves for five different concentrations of K_2-5′-GMP in aqueous solution are given in Figure 6. The 0.57, 0.45, 0.34, and 0.23 M solutions show a band with a maximum at ca. 115 cm^{-1}, for which the intensity relative to the water band at 180 cm^{-1} decreases with decreasing concentration of K_2-5′-GMP, and the band has completely disappeared in the 0.11 M solution. The solutions in Figure 6 all show a rather broad band appearing as a shoulder at ca. 70 cm^{-1}, but the intensity of this band is very low in the most concentrated solutions. With increasing concentration of K_2-5′-GMP the intensity of the band at 70 cm^{-1} decreases relative to the intensity of the band at 115 cm^{-1}.

The band at 115 cm^{-1} occurs for the sodium salt only at temperatures below ca. 30 °C, thus coinciding with the temperature region where several NMR studies[11-15] conclude that 5′-GMP is forming hydrogen-bonded self-associates. Different models for this self-association have been proposed, all involving stacks of planar hydrogen-bonded self-associates of 5′-GMP. The results presented here lends support to the conclusion based on NMR studies that the potassium ion is enhancing the self-association in the 5′-GMP solutions as compared to the sodium ion.

The temperature and concentration dependence for the $R(\bar{\nu})$ curves of K_2- and Na_2-5′-GMP in aqueous solution can be explained in terms of these self-association models. We assign the band at ca. 115 cm^{-1} to self-associates with hydrogen-bonded, coplanar purine rings. The band is rather sharp, which is anticipated for a well-defined binding between "planar" self-associates, but the line width should also be influenced by the number of molecules in a stack. In general a band should become sharper as the number of molecules in a stack increases. In the rest of this paper, the hydrogen-bonded self-associates with coplanar purine rings shall be referred to as HBS molecules.

The broad band with a maximum between 70 and 85 cm^{-1} is assigned to monomers or stacks of monomers. These looser associates shall be called MS (monomer stacked) molecules.

The $R(\bar{\nu})$ curves, obtained at different temperatures of 0.57 M K_2-5′-GMP solutions, in Figure 4 show that nearly all molecules are associated as HBS molecules below ca. 20 °C, because the intensity of the MS band at ca. 70 cm^{-1} is negligible in comparison to the 115-cm^{-1} band arising from HBS molecules. The band from MS molecules appears above ca. 20 °C, but the HBS molecules in the solution of the potassium salt still exist at 50 °C. Above ca. 50 °C precipitation occurred for the 0.57 M solution of the potassium salt, and it seems most likely that the solubility of the K_2-5′-GMP monomer is lower than for the corresponding sodium salt, which persists in solution under these conditions. The $R(\bar{\nu})$ curves of the sodium salt at different temperatures in Figure 3 reveal that the HBS molecules exist only at temperatures below 39 °C, because the 115-cm^{-1} band only show up at 25 °C and at lower temperatures. The MS molecules dominate even at low temperatures for the sodium salt.

A shift in maximum frequency from 85 cm^{-1} at −2 °C to 70 cm^{-1} at 51 °C is observed, Figure 3. Such a frequency shift might reflect a change in the stacking of monomers but could also be explained by anharmonicity in the intermolecular potential.

Figure 5 shows that the MS molecules at room temperature are the only species present in solutions of the sodium salt at concentrations lower than 0.3–0.4 M and still at the highest concentrations the MS molecules are dominant. Figure 6 shows that the HBS molecules are present in solutions of K_2-5′-GMP at a concentration of 0.23 M and higher, whereas this species is completely absent at the lowest concentrations (0.11 M), where only MS molecules are present. The precipitation in the 0.11 M solution of K_2-5′-GMP supports that the potassium salt of 5′-GMP monomer is less soluble than the sodium salt at pH ca. 8.

It is thus possible to assign the $R(\bar{\nu})$ curves of Na_2- and K_2-5′-GMP in weak basic solutions at different temperatures and concentrations to expected changes in equilibrium between only two different species: HBS and MS molecules. The potassium ions enhance the stability of the HBS molecules. A change in half-width of the band at 115 cm^{-1} might reflect the dependence upon temperature and concentration of the number of self-associated purine units in a stack. The half-width of the band seems to decrease with decreasing temperature or increasing concentration in accordance with an expected effect of stacking of HBS molecules.

Gels at pH Ca. 5. We have previously[6,9] used the $R(\bar{\nu})$ technique in a study of aqueous agarose and κ-carrageenan gels. Although the scattered intensity from the exciting line was extremely high, it was possible to obtain $R(\bar{\nu})$ curves of fairly good quality in the low-frequency region from ca. 20 cm^{-1}. At pH 5 the potassium and sodium salts of 5′-GMP form gels. Figure 7 shows $R(\bar{\nu})$ curves of aqueous gels of Na_2-5′-GMP at three different concentrations. All gels show a band with a maximum at 112 cm^{-1}, indicating that the self-association is very similar to that found for the HBS molecules, mentioned above. The band at 112 cm^{-1} gains intensity relative to the water band at 180 cm^{-1} in the more concentrated solutions. No bands corresponding to HBS molecules were present in solutions at corresponding concentrations of the sodium salt at slightly basic pH values.

The similarities of the bands between 110 and 120 cm^{-1} in the $R(\bar{\nu})$ curves of the gels of the sodium salt and the solutions of the potassium salt of 5′-GMP indicate that identical self-association

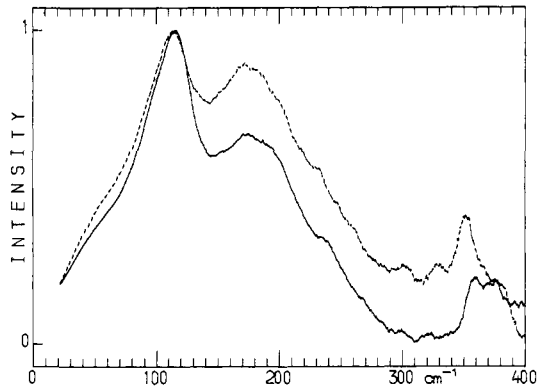

Figure 8. Full line: Smoothed $R(\nu)$ curve of a ca. 0.57 M aqueous solution of K_2-5′-GMP. Broken line: smoothed $R(\bar{\nu})$ curve of a ca. 0.55 M solution of deuterated K_2-5′-GMP in D_2O. Both solutions were investigated at pH ca. 8.

occurs. This does not imply that the binding of the sodium ions in the gel state is identical with the binding of the cations in the solution, because there is a difference in protonization of the phosphor group,[7] and this may play an important role for the self-association.

In comparison to the corresponding band in the slightly basic solutions of the potassium salt, the band at 112 cm^{-1} is sharper in the gels. The half-width is ca. 20 cm^{-1} in the gels and ca. 30 cm^{-1} in solutions at room temperature. This reflects most probably the fact that the number of purine rings in a stack is greater for the gel, and it seems reasonable to assume that this stacking of self-associated purine rings might result in the high viscosity (gel state) at this pH value.

Isotope Effects. In order to achieve a better knowledge of the physical origin of the modes giving rise to the low-frequency bands observed here, we compared the $R(\bar{\nu})$ curves of 5′-GMP dissolved in H_2O with the similar solutions of deuterated 5′-GMP in D_2O.

However, as shown in Figure 8 only small isotope effects are observed when comparing the $R(\bar{\nu})$ curves of K_2-5′-GMP in H_2O (0.57 M) with K_2-5′-GMP in D_2O (0.55 M). An identical conclusion could be drawn when comparing the similar solutions of Na_2-5′-GMP in H_2O and D_2O (not shown).

Although these observations might seem to contradict the interpretation that the modes involve hydrogen bonding, a similar isotopic independence have been reported for other hydrogen-bonded systems of which dimeric formic acid is a typical example.[21]

Thus a thorough discussion of the modes giving rise to these low-frequency bands shall wait until more experimental data has been gathered. In this context a study of other isotopic substituted species of 5′-GMP is of special interest.

Conclusion

This paper shows that it is possible to use the $R(\bar{\nu})$ representation in studying self-association of 5′-GMP in aqueous solutions as a function of cation (Na^+ or K^+) concentration, temperature, and pH. A band with a maximum at 110–120 cm^{-1} is assigned to self-associated 5′-GMP molecules with coplanar purine rings. Previous NMR results showing that this self-association is enhanced by potassium ions in solutions at pH ca. 8 are corroborated.[11-15]

The self-association of the sodium salt in the gel state at pH ca. 5 is more pronounced than in the corresponding solution of this salt at pH ca. 8. Although solutions of deuterium-substituted molecules (N–D and O–D) were investigated, a description of the modes giving rise to the low-frequency bands could not be achieved.

It is known that local changes in the environments of DNA molecules due to ions or proteins are likely to produce changes in conformation.[22] These conformational changes may give rise to changes in the low-frequency vibrational spectrum, and it is our hope that the $R(\bar{\nu})$ representation of the low-frequency Raman scattering in analogy with results in this paper can be used for more complicated systems of nucleic acids.

Acknowledgment. We wish to express our gratitude to the Danish Natural Science Research Council for partially financing the Raman equipment and to Dr. D. Christensen and Professor E. Praestgaard for helpful discussions.

Registry No. K_2-5′-GMP, 3254-39-5; Na_2-5′-GMP, 5550-12-9.

(21) Carlson, G. L.; Witkowski, R. E.; Fateley, W. G.; *Spectrochim Acta* **1966**, *22*, 1117–1123.
(22) Wang, A. H.-J.; Quigley, G. J.; Kolpak, F. J.; van der Marel, G.; van Boom, J. H.; Rich, A. *Science (Washington, D.C.)* **1981**, *211*, 171–176.

l-Canavanine, a Paradigm for the Structures of Substituted Guanidines

Alan Boyar and Richard E. Marsh*[1]

Contribution No. 6485 from the Arthur Amos Noyes Laboratory of Chemical Physics, California Institute of Technology, Pasadena, California 91125. *Received July 16, 1981*

Abstract: A crystal-structure study of the plant amino acid *l*-canavanine, the δ-oxa analogue of arginine, has been carried out. The zwitterionic molecule is protonated on the α-amino nitrogen atom; the neutral guanidine grouping is in the amino form, which seems to be preferred by all guanidine groups with electron-withdrawing substituents. Revised values of the various p*K*'s of canavanine and of canaline are reported, derived by reanalysis of the titration curves reported in 1935.

l-Canavanine, the δ-oxa analogue of *l*-arginine, is the principal nonprotein amino acid found in many species of the Lotoideae, also known as Papilionaceae or Fabaceae, a subfamily of the Leguminosae.[2] It is synthesized in the leaves and in the pod wall (pericarp) by a series of reactions which is postulated to be analogous to the arginine biosynthetic pathway and is stored in the seed where it may account for as much as 13% of the total dry weight. Canavanine functions as a source of nitrogen during germination and as a toxin to rodents and insects which might otherwise destroy the seeds. Canavanine is a substrate for nearly every enzyme for which arginine is also a substrate; it can competitively inhibit enzymes of arginine metabolism and is known

(1) To whom correspondence should be addressed.
(2) Bell, E. A.; Lakey, J. A.; Polhill, R. M. *Biochem. Syst. Ecol.* **1978**, *6*, 201–212.

0002-7863/82/1504-1995$01.25/0